Aromaticity

Deutsche Ausgabe: DOI: 10.1002/ange.201505766
Internationale Ausgabe: DOI: 10.1002/anie.201505766

Stepwise Reduction of 9,10-Bis(dimesitylboryl)anthracene

Yang Zheng, Jiao Xiong, Yangyang Sun, Xiaobo Pan, and Jincai Wu**

Abstract: *Stepwise reduction of 9,10-bis(dimesitylboryl)anthracene afforded an radical anion and a dianion, accompanied by stepwise changes of the aromaticity of the anthracene moiety. The radical has a planar semiquinoidal structure, while the dianion has a puckered quinoidal structure. The alteration of the geometries of the 9,10-bis(dimesitylboryl)anthracene upon reduction is rationalized by the nature of the bonding. These results have been confirmed by cyclic voltammetry, X-ray crystallography, NMR, EPR, and UV-vis-NIR spectroscopy, as well as DFT calculations.*

Because of the inherent electron deficiency, boron-based compounds can easily accept electrons to form reduced derivatives which possess unique chemical properties. They not only are important for understanding chemical bonding but also play essential roles in organic synthesis and functional materials.[1] Consequently, stabilization and isolation of their reduced species has become one of the most active research fields[1] in boron-based chemistry. Continuous efforts have led to the emergence of a number of stable boric radical anions[2] and anions,[3] which have been isolated and structurally characterized. However, as an important part of boron reduction chemistry, investigations for the reduction behaviors of diboryl-substituted compounds have just begun,[4,5] and so far only little (Scheme 1) is known about their structures and properties.[5]

Boron-containing π-conjugated systems have emerged as exciting subjects in contemporary organic materials chemistry,[6] such as, chemosensors for the detection of fluoride ions, nonlinear optical, charge-transport materials, as well as emitters in organic light-emitting devices. Although the structures of hundreds of neutral species are known, the corresponding reduced radical and dianion species together with X-ray structural data[5b,d] are rarely reported. Recently, Marder and co-workers reported a centrosymmetric semiquinoidal radical anion (**A**; Scheme 1) and a quinoidal dianion (**B**), which were obtained from a one- and two-electron reduction of 2,7-bis($BMes_2$)pyrene[5b], respectively. Braunschweig and co-workers reported a crystalline dianion[5d] (**D**) which exhibits a quinoidal structure featuring two B=C bonds, and is available by two-electron reduction of 2,5-bis(borolyl)thiophene. These interesting results display direct evidence for the formation of radical anions and dianions, and enhance the understanding of reduction chemistry of diboryl-substituted compounds. Moreover, the investigation of their carbon[7] and nitrogen[8] analogues demonstrated that the linker units of π-conjugated moieties significantly influence their electronic and crystal structures. Herein we chose the anthracene moiety as a bridging group, which is favorable for forming a good conjugated system with high delocalization, and present the stepwise reduction behavior of its diboryl-substituted derivative **1** (Scheme 2). We also describe the electronic and structural characteristics of the radical anion $\mathbf{1}^{\bullet-}$ and dianion $\mathbf{1}^{2-}$. The experimental results show that the former displays a semiquinoidal structure with perfectly planar geometry and two boron atoms participate in the aromatic system, while the latter possesses a puckered and distorted quinoidal structure accompanied by a loss of aromaticity in the central ring of the anthracene moiety.

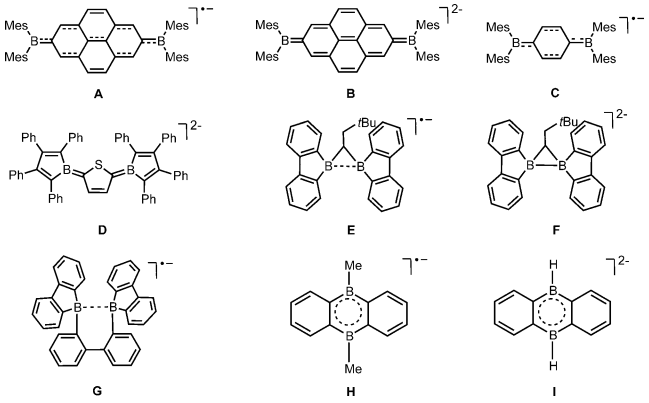

Scheme 1. Structurally characterized diboryl-substituted radical anions and dianions.

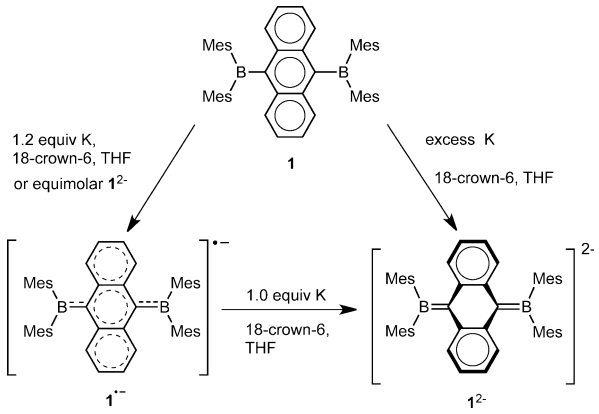

Scheme 2. Stepwise reduction of **1**.

[*] Y. Zheng, J. Xiong, Y. Sun, Prof. Dr. X. Pan, Prof. Dr. J. Wu
State Key Laboratory of Applied Organic Chemistry
Key Laboratory of Nonferrous Metal Chemistry and Resources Utilization of Gansu Province
College of Chemistry and Chemical Engineering
Lanzhou University, Lanzhou 730000 (P.R. China)
E-mail: boxb@lzu.edu.cn
wujc@lzu.edu.cn

Supporting information for this article is available on the WWW under http://dx.doi.org/10.1002/anie.201505766.

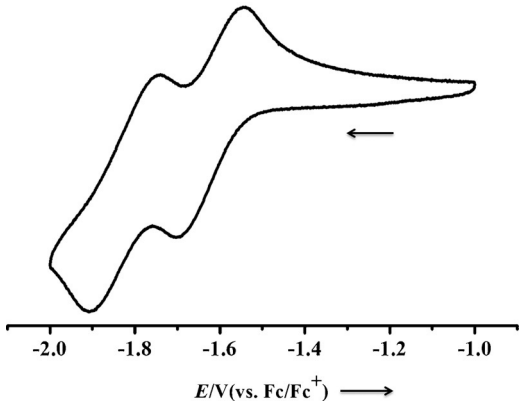

Figure 1. Cyclic voltammogram of **1** (1×10^{-3} M) in THF containing 0.1 M nBu$_4$NPF$_6$ and measured at 100 mV s^{-1} at room temperature.

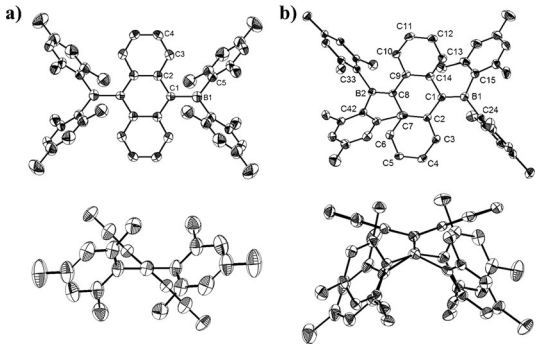

Figure 2. a) **1**$^{\bullet-}$ and b) **1**$^{2-}$ [top views (upper) and side views (lower)]. Thermal ellipsoids shown at 50% probability. All H atoms have been omitted for clarity. Selected bond lengths [Å] and angles [°]: in **1**$^{\bullet-}$, B1–C1 1.533(8), B1–C5 1.610(5), C1–C2 1.448(4), C2–C2a 1.426(6), C2–C3 1.418(4), C3–C4 1.360(5), C4–C4a 1.384(7), C1–B1-C5 122.3(2); C1-B1-C5a 122.3(2), C5-B1-C5a 115.4(5), C2-C1-C2a 115.8(4), C2-C1-B1 122.1-(2), C2-C1-B1 122.1(2); in **1**$^{2-}$: B1–C1 1.486(7), B1–C15 1.624(7), B1–C24 1.639(7), B2–C8 1.483(6), B2–C33 1.639(6), B2–C42 1.626(6), C1–C2 1.476(6), C1–C14 1.491(6), C2–C3 1.402(6), C2–C7 1.440(6), C3–C4 1.402(7), C4–C5 1.391(6), C5–C6 1.396(6), C6–C7 1.399(6), C7–C8 1.475(6), C8–C9 1.478(6), C9–C10 1.415(6), C9–C14 1.424(6), C10–C11 1.395(7), C11–C12 1.372(7), C12–C13 1.385(6), C13–C14 1.393(6); C1-B1-C15 122.4(4), C1-B1-C24 125.6(4), C15-B1-C24 111.7(4), C8-B2-C42 123.1(4), C8-B2-C33 127.0(4), C42-B2-C33 109.7(3), B1-C1-C14 121.2-(4), C2-C1-B1 127.1(4), C2-C1-C14 111.6(4), C7-C8-C9 112.1(4), C7-C8-B2 120.8(4), C9-C8-B2 126.8(4).

9,10-Bis(dimesitylboryl)anthracene (**1**) was prepared according to literature methods.[9] The cyclic voltammetry of **1** in THF, with nBu$_4$NPF$_6$ as a supporting electrolyte, shows two quasi-reversible reduction waves at $E_{1/2}=-1.62$ and -1.82 V vs. Fc/Fc$^+$ (Figure 1; see Figure S1 in the Supporting Information), and is comparable to that of 9,10-bis(di-9-anthrylboryl)anthracene ($E_{1/2}=-1.61$ and -1.76 V vs. Fc/Fc$^+$),[9c] thus indicating that the radical anion **1**$^{\bullet-}$ and dianion **1**$^{2-}$ may be stable under these experimental conditions. The separation of the first and second reduction waves ($\Delta E=$ 0.20 V) is smaller than that of 4,4′-bis(BMes$_2$)-1,1′-biphenyl[4b] ($\Delta E=0.25$ V) and 2,7-bis(BMes$_2$)pyrene[5b] ($\Delta E=0.28$ V), thus suggesting some degree of charge delocalization between two borolyl fragments across the anthracene bridge. Addition of excess potassium metal to a yellow THF solution of **1** and 18-crown-6 (18-C-6) leads to a red compound [K(18-C-6)]$^+$[K(THF)$_2$(18-C-6)]$^+$·**1**$^{2-}$ (Scheme 2) in a moderate yield within one day. The compound **1**$^{2-}$ is EPR silent in THF solution and gives perfectly well-resolved NMR spectra with chemical-shift values in typical ranges of diamagnetic species ([D$_8$]THF). The ^{11}B NMR resonance (see Figure S2) of **1**$^{2-}$ appears at $\delta=37.4$ ppm, which is close to those in compounds **B**,[5b] **D**,[5d] and some previously reported borataalkenes[10] (see Table S2). In the ^{1}H and ^{13}C NMR spectra (see Figures S3 and S4), all ^{1}H and ^{13}C NMR chemical shifts for **1**$^{2-}$ were completely assigned. The ^{1}H NMR resonances of the anthracene group of **1**$^{2-}$ at $\delta=6.68$ and 5.70 ppm are shifted upfield by $\delta=1.82$ and 1.05 ppm, respectively, when compared to that of **1**. This shift is consistent with the loss of aromaticity of the central ring in the anthracene moiety. A comproportionation reaction between equimolar amounts of [K(18-C-6)]$^+$[K-(THF)$_2$(18-C-6)]$^+$·**1**$^{2-}$ and **1** (Scheme 2) in THF at room temperature provides dark green solution of **1**$^{\bullet-}$. The EPR spectrum (see Figure S5) of **1**$^{\bullet-}$ in THF confirmed the existence of the radical anion **1**$^{\bullet-}$. The absence of resolved hyperfine coupling is likely due to the many different couplings arising from a highly delocalized structure[2b,5b,11] in which the spin density of the unpaired electron is distributed over the anthracene moiety and BMes$_2$ units.

Crystals suitable for X-ray crystallographic studies were obtained by cooling solutions of **1**$^{\bullet-}$ and **1**$^{2-}$ in THF. Figures 2a and b display the solid-state structures of [K(THF)$_2$(18-C-6)]$^+$·**1**$^{\bullet-}$ and [K(18-C-6)]$^+$[K(THF)$_2$(18-C-6)]$^+$·**1**$^{2-}$, respectively. A list of their important structure parameters, as well as those of **1**, is given in Table S3. [K(THF)$_2$(18-C-6)]$^+$[**1**$^{\bullet-}$] consists of a discrete cation [K(THF)$_2$(18-C-6)]$^+$ and radical anion **1**$^{\bullet-}$. Whereas for [K(18-C-6)]$^+$[K(THF)$_2$(18-C-6)]$^+$·**1**$^{2-}$, except for the fully separated cation [K(THF)$_2$(18-C-6)]$^+$, the other [K(18-C-6)]$^+$ interacts with aromatic ring through a cation–π interaction (see Figure S6). In all the structures, B1 (or B2) and C1 (or C8) adopt a trigonal-planar geometry. The B1–C1 (or B2–C8) bond (see Table S3) undergoes an obvious shortening on going from **1** to **1**$^{\bullet-}$ to **1**$^{2-}$, while B1(or B2)–C(Mes) and C1(or C8)–C(Ar) (see Table S3) significantly lengthen. Similar trends have been found in the reducing processes of the acridinium borane cation,[2e,3e] 2,7-bis(BMes$_2$)pyrene,[5b] and 2,5-bis(borolyl)thiophene.[5d]

For **1**$^{\bullet-}$, the B1–C1 bond length [1.533(8) Å] is between a B–C ($\approx$1.59 Å) bond measured in bulky triarylboranes and a B=C bond observed in borataalkenes.[5b,d,10] The dihedral angle formed by the B–C3 trigonal plane [B1 (or B2) with the adjacent carbon atoms] and the anthracene moiety decrease on going from **1** to **1**$^{\bullet-}$ (53.0° in **1**, 41.9° in **1**$^{\bullet-}$; see Figure S7). The observed bond length alternation (BLA)[5b,8a] of the anthracene moiety (0.030 Å) testifies to a semiquinoidal structure, thus indicating strong conjugation between the boron centers and the anthracene bridge, and decreased aromaticity of the anthrance moiety upon injection of one electron into the parent **1**. For **1**$^{2-}$, the structure clearly shows two B=C bonds [B1-C1 1.486(7) Å, B2-C8 1.483(6) Å] which are slightly shorter than the B=C bond in **B**[5b] [1.510(3) Å]

and **D**[5d] [1.523(4) and 1.509(4) Å], but in the range of known B=C(aryl) double bonds (see Table S4).[10] The formation of these B=C bonds causes the significant lengthening of C1(or C8)–C (Ar) (see Table S3) bonds, which do not possess the double-bond character of aromatic ring. Thus the aromaticity is completely lost in the central ring of the anthracene moiety. In another word, the injection of two electrons into the parent **1** leads to the formation of the puckered geometry and the distorted quinoidal structure of $\mathbf{1}^{2-}$ (Figure 2b; see Figure S8), simultaneously giving rise to the change of aromaticity. Moreover, the BLA of the anthracene unit (0.022 Å) is significantly decreased compared with that of $\mathbf{1}^{\bullet-}$ and the recently reported **B** (0.058 Å),[5b] thus indicating a decreased quinoidal structure. This result is also different from its isoelectronic nitrogen analogue reported by Wang and coworkers,[8a] wherein the analogue has a planar geometry and possess a characteristic resonance structure which is between that of an open-shell diradical and a closed-shell quinonoid form.

To further understand the experimental results, we carried out DFT calculations[12] for the model $\mathbf{1}_{opt}$ ($Mes_2BC_{14}H_8BMes_2$) and its reduced species $\mathbf{1}^{\bullet-}{}_{opt}$ and $\mathbf{1}^{2-}{}_{opt}$. The geometry optimizations were performed at the (U)B3LYP/6-31G(d) level of theory. The calculated structural parameters of $\mathbf{1}_{opt}$ and its reduced species are in good agreement with those of X-ray experimental data (see Table S3). Consistent with the experimental data, the B1–C1 (or B2–C8) bond becomes shorter, whereas the B1 (or B2)–C(Mes) and C1(or C8)–C(Ar) bond distances become longer when going from $\mathbf{1}_{opt}$ to $\mathbf{1}^{\bullet-}{}_{opt}$ to $\mathbf{1}^{2-}{}_{opt}$. The alteration of the B–C and C–C bond lengths can be explained by the nature of B–C and C–C bonding. As shown in Figure 3, the LUMO of $\mathbf{1}_{opt}$ is mainly π (B1=C1 and B2=C8), an in-phase combination of p orbitals of boron and carbon atoms. The π (B1=C1 and B2=C8) orbital (LUMO; Figure 3a) in $\mathbf{1}_{opt}$ is empty, but it is singly occupied in $\mathbf{1}^{\bullet-}{}_{opt}$ (SOMO; Figure 3b) and doubly occupied in $\mathbf{1}^{2-}{}_{opt}$ (HOMO; Figure 3c). The increase in the occupation of the π (B1=C1 and B2=C8) orbital leads to a shortening of the B1–C1 (or B2–C8) bond, and finally causes puckering of the anthracene moiety accompanied by the changed aromaticity of the anthracene moiety. The calculated bond order[12] (Mayer 0.90, Wiberg 0.98 for $\mathbf{1}_{opt}$; Mayer 1.12, Wiberg 1.17 for $\mathbf{1}^{\bullet-}{}_{opt}$; Mayer 1.44, Wiberg 1.48 for $\mathbf{1}^{2-}{}_{opt}$) of B–C further supports the sequential changes of experimental B–C bond and the formation of B=C bond. These bond orders are smaller than the corresponding theoretical values, possibly because of the polarization of the B–C bond.[3e] In addition, the calculated spin density (Figure 3d) of $\mathbf{1}^{\bullet-}{}_{opt}$ is mainly localized on boron atoms ($0.266\,e \times 2$) and the adjacent carbon atoms ($0.142\,e \times 2$) of the anthracene moiety. Together with the experimental data, these calculated results suggest that the reduction of **1** leads to the formation of the planar semiquinoidal structure $\mathbf{1}^{\bullet-}$ and puckered quinoidal structure $\mathbf{1}^{2-}$.

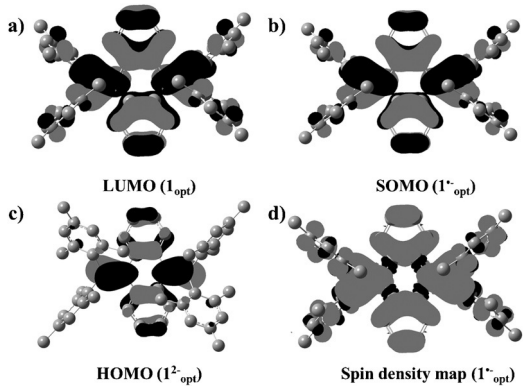

Figure 3. a) LUMO of $\mathbf{1}_{opt}$. b) SOMO of $\mathbf{1}^{\bullet-}{}_{opt}$. c) HOMO of $\mathbf{1}^{2-}{}_{opt}$. d) Spin density map of $\mathbf{1}^{\bullet-}{}_{opt}$.

The UV-vis-NIR absorption spectra of $\mathbf{1}^{2-}$ and $\mathbf{1}^{\bullet-}$ in THF show a maximum absorption peak at $\lambda = 776$ and 952 nm, respectively (see Figure S9). Judging from the time-dependent DFT (TD-DFT) calculation,[13] the maximum absorption of $\mathbf{1}^{2-}{}_{opt}$ [PBEPBE/6-311G(d,p) level] is assigned to HOMO→LUMO (49%), HOMO→LUMO+2 (25%), and HOMO→LUMO+4 (25%) electronic transitions (see Figure S10), while the maximum absorption of $\mathbf{1}^{\bullet-}{}_{opt}$ (UCAM-B3LYP/6-311G(d,p)) is assigned to HOMO(α)→LUMO(α) electron transitions (see Figure S11).

In conclusion, we have described the stabilization and characterization of the radical anion $\mathbf{1}^{\bullet-}$ and dianion salt $\mathbf{1}^{2-}$. The former shows a planar semiquinoidal structure while the latter has a puckered and distorted quinoidal structure. According to the experimental and computational results, a clear shortening of boron–carbon π bond, as well as changes of aromaticity of the anthracene moiety were verified upon one- and two-electron reduction. Further studies on the chemical reactivities of these reduced species are under way.

Acknowledgements

This work has been supported by the National Natural Science Foundation of China (No. 21271092 and 21401161) and the Fundamental Research Funds for the Central Universities. We also sincerely appreciate Dr. Xingyong Wang and Yuanting Su for their useful discussions and suggestions.

Keywords: aromaticity · boron · density functional calculations · radicals · reduction

How to cite: *Angew. Chem. Int. Ed.* **2015**, *54*, 12933–12936
Angew. Chem. **2015**, *127*, 13125–13128

[1] a) J. Fossey, D. Lefort, J. Sorba, *Free Radicals in Organic Chemistry*, Wiley, New York, **1995**; b) F. Gerson, W. Huber, *Electron Spin Resonance Spectroscopy of Organic Radicals*, Wiley-VCH, New York, **2003**; c) P. P. Power, *Chem. Rev.* **2003**, *103*, 789–810; d) W. Kaim, N. S. Hosmane, S. Záliš, J. A. Maguire, W. N. Lipscomb, *Angew. Chem. Int. Ed.* **2009**, *48*, 5082–5091; *Angew. Chem.* **2009**, *121*, 5184–5193; e) C. D. Martin, M. Soleilhavoup, G. Bertrand, *Chem. Sci.* **2013**, *4*, 3020–3030; f) T. Chivers, J. Konu in *Comprehensive Inorganic Chemistry II: From Elements to Applications*, *Vol. 1* (Ed.: T. Chivers), Elsevier, Amsterdam, **2013**, p. 349; g) H. Braunsch-

weig, R. D. Dewhurst, *Angew. Chem. Int. Ed.* **2013**, *52*, 3574 – 3583; *Angew. Chem.* **2013**, *125*, 3658 – 3667.

[2] See, for example: a) M. M. Olmstead, P. P. Power, *J. Am. Chem. Soc.* **1986**, *108*, 4235 – 4236; b) W. J. Grigsby, P. P. Power, *Chem. Commun.* **1996**, 2235 – 2236; c) V. Lorenzen, W. Preetz, *Z. Naturforsch. B* **1997**, *52*, 565 – 572; d) W. J. Grigsby, P. P. Power, *Chem. Eur. J.* **1997**, *3*, 368 – 375; e) C.-W. Chiu, F. P. Gabbaï, *Angew. Chem. Int. Ed.* **2007**, *46*, 1723 – 1725; *Angew. Chem.* **2007**, *119*, 1753 – 1755; f) V. J. Richards, A. L. Gower, J. E. H. B. Smith, S. Davies, D. Lahaye, A. G. Slater, W. Lewis, A. J. Blake, N. R. Champness, D. L. Kays, *Chem. Commun.* **2012**, *48*, 1751 – 1753; g) H. Braunschweig, V. Dyakonov, J. O. C. Jimenez-Halla, K. Kraft, I. Krummenacher, K. Radacki, A. Sperlich, J. Wahler, *Angew. Chem. Int. Ed.* **2012**, *51*, 2977 – 2980; *Angew. Chem.* **2012**, *124*, 3031 – 3034; h) P. Bissinger, H. Braunschweig, A. Damme, C. Hörl, I. Krummenacher, T. Kupfer, *Angew. Chem. Int. Ed.* **2015**, *54*, 359 – 362; *Angew. Chem.* **2015**, *127*, 366 – 369.

[3] See, for example: a) A. Moezzi, M. M. Olmstead, P. P. Power, *J. Am. Chem. Soc.* **1992**, *114*, 2715 – 2717; b) P. P. Power, *Inorg. Chim. Acta* **1992**, *198*, 443 – 447; c) A. Moezzi, R. A. Bartlett, P. P. Power, *Angew. Chem. Int. Ed. Engl.* **1992**, *31*, 1082 – 1083; *Angew. Chem.* **1992**, *104*, 1075 – 1076; d) H. Nöth, J. Knizek, W. Ponikwar, *Eur. J. Inorg. Chem.* **1999**, 1931 – 1937; e) C.-W. Chiu, F. P. Gabbaï, *Angew. Chem. Int. Ed.* **2007**, *46*, 6878 – 6881; *Angew. Chem.* **2007**, *119*, 7002 – 7005.

[4] For spectroscopy studies on diboryl-substituted reduced species, see: a) J. D. Hoefelmeyer, F. G. Gabbaï, *J. Am. Chem. Soc.* **2000**, *122*, 9054 – 9055; b) J. Fiedler, S. Zališ, A. Klein, F. M. Hornung, W. Kaim, *Inorg. Chem.* **1996**, *35*, 3039 – 3043; c) A. Rajca, S. Rajca, S. R. Desai, *J. Chem. Soc. Chem. Commun.* **1995**, 1957 – 1958; d) A. Schulz, W. Kaim, *Chem. Ber.* **1989**, *122*, 1863 – 1868; e) W. Kaim, A. Schulz, *Angew. Chem. Int. Ed. Engl.* **1984**, *23*, 615 – 616; *Angew. Chem.* **1984**, *96*, 611 – 612; f) R. L. Hudson, F. Williams, *J. Am. Chem. Soc.* **1977**, *99*, 7714 – 7716.

[5] For structurally characterized of diboryl-substituted reduced species, see: a) A. Hübner, T. Kaese, M. Diefenbach, B. Endeward, M. Bolte, H.-W. Lerner, M. C. Holthausen, M. Wagner, *J. Am. Chem. Soc.* **2015**, *137*, 3705 – 3714; b) L. Ji, R. M. Edkins, A. Lorbach, I. Krummenacher, C. Brückner, A. Eichhorn, H. Braunschweig, B. Engels, P. J. Low, T. B. Marder, *J. Am. Chem. Soc.* **2015**, *137*, 6750 – 6753; c) A. Hübner, A. M. Diehl, M. Diefenbach, B. Endeward, M. Bolte, H.-W. Lerner, M. C. Holthausen, M. Wagner, *Angew. Chem. Int. Ed.* **2014**, *53*, 4832 – 4835; *Angew. Chem.* **2014**, *126*, 4932 – 4935; d) H. Braunschweig, V. Dyakonov, B. Engels, Z. Falk, C. Hörl, J. H. Klein, T. Kramer, H. Kraus, I. Krummenacher, C. Lambert, C. Walter, *Angew. Chem. Int. Ed.* **2013**, *52*, 12852 – 12855; *Angew. Chem.* **2013**, *125*, 13088 – 13092; e) A. Lorbach, M. Bolte, H.-W. Lerner, M. Wagner, *Organometallics* **2010**, *29*, 5762 – 5765; f) P. Müller, S. Huck, H. Köppel, H. Pritzkow, W. Siebert, *Z. Naturforsch. B* **1995**, *50*, 1476 – 1484.

[6] See, for example: a) F. Jäkle, *Chem. Rev.* **2010**, *110*, 3985 – 4022; b) C. R. Wade, A. E. J. Broomsgrove, S. Aldridge, F. P. Gabbaï, *Chem. Rev.* **2010**, *110*, 3958 – 3984; c) S. Yamaguchi, A. Wakamiya, *Pure Appl. Chem.* **2006**, *78*, 1413 – 1424; d) C. D. Entwistle, T. B. Marder, *Chem. Mater.* **2004**, *16*, 4574 – 4585; e) C. D. Entwistle, T. B. Marder, *Angew. Chem. Int. Ed.* **2002**, *41*, 2927 – 2931; *Angew. Chem.* **2002**, *114*, 3051 – 3056; f) S. Yamaguchi, S. Akiyama, K. Tamao, *J. Am. Chem. Soc.* **2001**, *123*, 11372 – 11375; and references therein.

[7] Selected examples: a) L. K. Montgomery, J. C. Huffman, E. A. Jurczak, M. P. Grendze, *J. Am. Chem. Soc.* **1986**, *108*, 6004 – 6011; b) A. Rajca, *Chem. Rev.* **1994**, *94*, 871 – 893; c) W. W. Porter III, T. P. Vaid, A. L. Rheingold, *J. Am. Chem. Soc.* **2005**, *127*, 16559 – 16566; d) T. Kubo, A. Shimizu, M. Sakamoto, M. Uruichi, K. Yakushi, M. Nakano, D. Shiomi, K. Sato, T. Takui, Y. Morita, K. Nakasuji, *Angew. Chem. Int. Ed.* **2005**, *44*, 6564 – 6568; *Angew. Chem.* **2005**, *117*, 6722 – 6726; e) C. Lambert, *Angew. Chem. Int. Ed.* **2011**, *50*, 1756 – 1758; *Angew. Chem.* **2011**, *123*, 1794 – 1796; f) Z. Sun, Q. Ye, C. Chi, J. Wu, *Chem. Soc. Rev.* **2012**, *41*, 7857 – 7889; g) M. Abe, *Chem. Rev.* **2013**, *113*, 7011 – 7088; h) Z. Sun, Z. Zeng, J. Wu, *Acc. Chem. Res.* **2014**, *47*, 2582 – 2591.

[8] a) Y. Su, X. Wang, Y. Li, Y. Song, Y. Sui, X. Wang, *Angew. Chem. Int. Ed.* **2015**, *54*, 1634 – 1637; *Angew. Chem.* **2015**, *127*, 1654 – 1657; b) Y. Su, X. Wang, X. Zheng, Z. Zhang, Y. Song, Y. Sui, Y. Li, X. Wang, *Angew. Chem. Int. Ed.* **2014**, *53*, 2857 – 2861; *Angew. Chem.* **2014**, *126*, 2901 – 2905; c) X. Zheng, X. Wang, Y. Qiu, Y. Li, C. Zhou, Y. Sui, Y. Li, J. Ma, X. Wang, *J. Am. Chem. Soc.* **2013**, *135*, 14912 – 14915; d) K. Kamada, S. Fuku-en, S. Minamide, K. Ohta, R. Kishi, M. Nakano, H. Matstuzaki, H. Okamoto, H. Higashikawa, K. Inoue, S. Kojima, Y. Yamamoto, *J. Am. Chem. Soc.* **2013**, *135*, 232 – 241; e) S. Zheng, S. Barlow, C. Risko, T. L. Kinnibrugh, V. N. Khrustalev, S. C. Jones, M. Y. Antipin, N. M. Tucker, T. V. Timofeeva, V. Coropeanu, J. Brédas, S. R. Marder, *J. Am. Chem. Soc.* **2006**, *128*, 1812 – 1817.

[9] a) C. Förster, W. Seichter, A. Schwarzer, E. Weber, *Supramol. Chem.* **2010**, *22*, 571 – 581; b) Z. Yuan, N. J. Taylor, R. Ramachandran, T. B. Marder, *Appl. Organomet. Chem.* **1996**, *10*, 305 – 316; c) S. Yamaguchi, S. Akiyama, K. Tamao, *J. Am. Chem. Soc.* **2000**, *122*, 6335 – 6336.

[10] a) P.-Y. Feng, Y.-H. Liu, T.-S. Lin, S.-M. Peng, C.-W. Chiu, *Angew. Chem. Int. Ed.* **2014**, *53*, 6237 – 6240; *Angew. Chem.* **2014**, *126*, 6351 – 6354; b) J. Möbus, G. Kehr, C. G. Daniliuc, R. Fröhlich, G. Erker, *Dalton Trans.* **2014**, *43*, 632 – 638; c) J. Bauer, H. Braunschweig, C. Hörl, K. Radacki, J. Wahler, *Chem. Eur. J.* **2013**, *19*, 13396 – 13401; d) J. D. Hoefelmeyer, S. Solé, F. P. Gabbaï, *Dalton Trans.* **2004**, 1254 – 1258; e) M. M. Olmstead, P. P. Power, K. J. Weese, *J. Am. Chem. Soc.* **1987**, *109*, 2541 – 2542; f) R. A. Bartlett, P. P. Power, *Organometallics* **1986**, *5*, 1916 – 1917.

[11] a) A. Lichtblau, W. Kaim, A. Schulz, T. Stahl, *J. Chem. Soc. Perkin Trans. 2* **1992**, 1497 – 1501; b) T. Matsumoto, F. P. Gabbaï, *Organometallics* **2009**, *28*, 4252 – 4253.

[12] All calculations were performed with the Gaussian 09 program suite (Revision A.01). Frequency calculations were carried out to confirm that all optimized geometries correspond to energy minima. **1** was optimized on the B3LYP/6-31G(d) level. $\mathbf{1}^{2<M->}$ and $\mathbf{1}^{\bullet-}$ were optimized on B3LYP/6-31G(d) level (restricted formalism for $\mathbf{1}^{2-}$, and unrestricted for $\mathbf{1}^{\bullet-}$). The molecular orbitals and spin densities were calculated at the corresponding optimized geometries. Mayer and Wiberg bond orders were also calculated at the same level with the Multiwfn program. See Supporting Information for geometries and coordinates.

[13] The UV-vis-NIR absorption spectrum for $\mathbf{1}^{2-}{}_{opt}$ was calculated using time-dependent DFT (TD-DFT) method at PBEPBE/6-311G(d,p) level of theory, whereas UCAM-B3LYP/6-311G(d,p) for $\mathbf{1}^{\bullet-}{}_{opt}$. Fifty singlet transitions were calculated for each compound.

Received: June 23, 2015
Revised: July 22, 2015
Published online: September 8, 2015

